



Testing exact vacuum mirror symmetry toward matter

ALAN SCHWARTZ

ABSTRACT

Achiral spacetime curvature and chiral spacetime torsion are functionally equivalent. Predicted torsion background angular momentum divergences have not been observed. Rigid polyatomic opposite shoes divergently fitting a trace vacuum left foot are untested. Geometric Eötvös, calorimetry, and molecular rotation temperature experiments are presented. Interactions of torsion trace vacuum chiral anisotropy selective to hadronic matter are measurable, consequential, and more compatible with prior observations than postulated exact vacuum achiral isotropy. (PACS: 04.80.Cc, 11.30.Er)

READ REVIEWS

WRITE A REVIEW

CORRESPONDENCE:
xenophage@gmail.com

DATE RECEIVED:
June 11, 2015

KEYWORDS:
equivalence principle, chirality,
gravitation, anisotropy

© Schwartz This article is distributed under the terms of the [Creative Commons Attribution 4.0 International License](https://creativecommons.org/licenses/by/4.0/), which permits unrestricted use, distribution, and redistribution in any medium, provided that the original author and source are credited.



1. INTRODUCTION

Postulating the Equivalence Principle (EP) elevates special relativity to general relativity (GR): All local matter identically vacuum free falls along parallel-displaced minimum action trajectories. No measurable property of matter causes divergence. Composition and polarized spin Eötvös experiments; Nordtvedt effect and lunar laser ranging; pulsar binary systems with pulsars, white dwarfs, or solar stars all validate GR to limits of measurement in all predictions for all measurable properties and fields — classical, quantum mechanical, relativistic, and gravitational (strong EP).

Einstein-Cartan-Kibble-Sciama gravitation (ECKS) contracts to GR if the EP is exactly true (achiral spacetime curvature). ECKS theory contains unobserved angular momentum EP violations given chiral spacetime torsion. Geometric chirality is an absolutely discontinuous symmetry outside Noether's theorems. Geometric chirality cannot be measured. Chiral spacetime torsion is a vacuum trace left foot. Rigid polyatomic opposite shoes geometrically test spacetime geometry to confirm or falsify an EP footnote. Examples for three of five test classes are presented.

2. BOUNDARY CONDITIONS

Massless boson photons detect no vacuum refraction, dispersion, dissipation, dichroism, or gyrotropy. Postulate contingent vacuum symmetries are exactly true for fermionic matter (quarks, hadrons). Parity violations, symmetry breakings, chiral anomalies, baryogenesis, biological homochirality, Chern-Simons repair of Einstein-Hilbert action are consistent with vacuum trace chiral anisotropy acting only upon hadrons.

Noether's theorems couple exact vacuum isotropy with conservation of angular momentum. Vacuum trace chiral anisotropy selective to hadronic matter leaks as MoND's $1.2 \times 10^{-10} \text{ m/s}^2$ Milgrom acceleration. Dark matter curve-fits the Tully-Fisher relation. Dark matter is empirically undetected. Planck satellite's 5.47:1 (dark matter):(baryonic matter) mass:mass ratio, including sun concentration, appears as less than 1.7×10^{-10} solar masses of dark matter within Saturn's orbital sphere. Without solar dark matter concentration, less than 6.8×10^{-11} solar masses of dark matter (N. P. Pitjeve, 2013).

Geometric chirality is easily observed (no S_n symmetries) and easily calculated with QCM software

(Petitjohn, 1999) but it cannot be measured. α -Quartz and γ -glycine single crystals have calculated $\text{CHI} = 1$ $\text{DSI} = 0$ $\text{COR} = 1$ maximum geometric chirality, but it cannot be measured. Silver thiogallate, AgGaS_2 in *achiral* space group $I\bar{4}2d$ (#122), rotates plane polarized sodium D-line light $522^\circ/\text{mm}$ along [100] at 497.4 nm (J. Etxebarria, 2000). $P3121$ (#152) quartz and $P3221$ (#154) berlinite, mirror image atomic helices, are both levorotatory (A. M. Glazer, 1986). Achiral PhCOCH_3 impurity changes resolved PhCH(OH)CH_3 optical rotation (S. Yamaguchi, 1973). CIP notation flips within unchanged geometry, L-(2*S*)-alanine but L-(2*R*)-cysteine. Solution specific rotations ignore atomic mass distribution, Fig. 1 and Table 1.

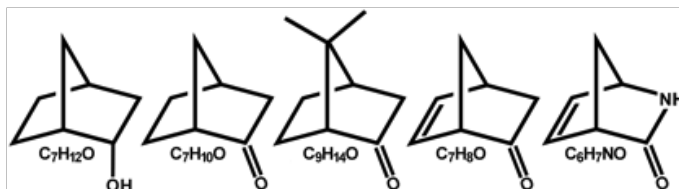


Figure 1: Similar absolute configuration mass distribution chiral molecules

Table 1: Uncoupled mass distributions and specific rotations

Formula	Formal name	Specific rotation [α]D ($^\circ\text{-cm}^3/\text{dm-g}$)
$\text{C}_7\text{H}_{12}\text{O}^{\text{a}}$	(1 <i>R</i> ,2 <i>S</i> ,4 <i>S</i>)-bicyclo[2.2.1]heptan-2-ol	-2.3
$\text{C}_7\text{H}_{10}\text{O}^{\text{b}}$	(1 <i>R</i> ,4 <i>S</i>)-bicyclo[2.2.1]heptan-2-one	-29.8
$\text{C}_9\text{H}_{14}\text{O}^{\text{c}}$	(1 <i>R</i> ,4 <i>R</i>)-7,7-dimethylbicyclo[2.2.1]heptan-2-one	+73.9
$\text{C}_7\text{H}_8\text{O}^{\text{d}}$	(1 <i>S</i> ,4 <i>S</i>)-bicyclo[2.2.1]hept-5-en-2-one	-1146.
$\text{C}_6\text{H}_7\text{NO}^{\text{e}}$	(1 <i>R</i> ,4 <i>S</i>)-2-azabicyclo[2.2.1]hept-5-en-2-one	-565.

^aEuropean patent EP0801135 A1 (1997); ^{b,d}*J. Phys. Chem. A*, 2006: **110**(51), 13995 - 14002, doi:10.1021/jp0655221;

^c*J. Org. Chem.*, 1974: **39**(12), 1653 - 1656, doi:10.1021/jo00925a011; *Ann. Acad. So. Fenn, Ser A2*, 1961: 105(1), 22; ^e*J. Chem. Soc., Chem. Commun.*, 1990: 1120 - 1121, doi:10.1039/C39900001120

3. DROPPING OPPOSITE SHOES

Opposite shoes embed within chiral vacuum background (mount a left foot) with different energies. They vacuum free fall along non-identical minimum action trajectories, exhibiting EP violation. Achiral symmetry plus lattice discretization fails (H.B. Nielsen, 1981). Periodic lattices and quantum spacetime attack vacuum isotropy (Fritz, 2013). Crystallography's opposite shoes are visually and chemically identical, single crystal test masses in enantiomorphic space groups (Souvignier, 2003) (A. F. Palistrant, 1991). Two examples are $P3121$ versus $P3221$ α -quartz or $P31$ (#144) versus $P32$ (#145) γ -glycine. Eötvös experiments are 5×10^{-14} difference/average sensitive (T. A. Wagner, 2012). Composition-nulled controls are α -quartz versus amorphous fused silica, γ -glycine versus achiral $P21/n$ (#14, non-standard setting) α -glycine.

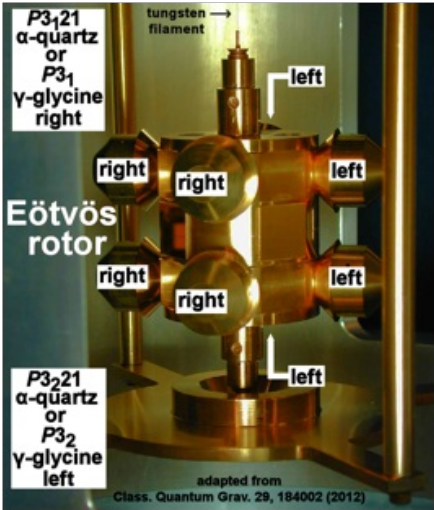


Figure 2: Two geometric Eötvös experiments

The α -quartz unit cell is 0.113 nm^3 volume. 40 grams net as 8 single crystal test masses compare 6.68×10^{22} pairs of opposite shoes (pairs of 9-atom enantiomorphic unit cells, the test mass array cube's opposite vertical sides), Fig.2.

Composition and polarized spin Eötvös experiments' net active mass fractions are negligible. Titanium versus beryllium nuclear binding energy is 0.0023974 net active mass fraction (weighted isotopic abundances), the largest relative divergence composition contrast compatible with hard vacuum. Theoretical 100% polarized spin (empirically antiferromagnetic, space group $Fm\bar{3}m$ (#225)) octahedral MnO lattice, five parallel unpaired electrons/Mn(II) in the least massive formula unit, is 0.000038669 net active mass fraction, Eq. (1).

$$5(5.485799 \times 10^{-4} \text{ amu/electron}) / (54.93805 \text{ amu/Mn} + 15.994915 \text{ amu/O}) \tag{1}$$

Net active mass fractions in any geometric test of spacetime geometry, nucleus' relative positions in space , are shown in Table 2. They are 400 times the net active mass fraction of the most divergent composition Eötvös experiments.

Table 2: Eötvös experiment net active mass fractions

Net active mass fraction	Space groups	Single crystal	Material
0.999708	$P31$	γ -glycine	
	$P32$		
0.999713	$P3121$	benzil	
	$P3221$		
0.999726	$P3121$	α -quartz	
	$P3221$		
0.999775	$P3121$	tellurium	

*P*3221

0.0023974

Be versus Ti

0.000038669

MnO undecaplet

4. MELTING OPPOSITE SHOES

An Eötvös experiment is geometry-conserving. A calorimetry experiment is geometry-destroying. It melts opposite shoes into identical achiral socks, all on a vacuum left foot. Divergent chiral energies of fit transform into a common achiral state. A time-varying EP violation, Earth's inertial rotation versus gravitational orbit, is added to a constant differential chiral vacuum background insertion energy over a 24-hour day.

The geometric calorimetric test masses are 94.85 °C melting point, space group *P*3121 versus *P*3221 single crystal benzil, Fig. 3. QCM software calculates CHI = 1 DSI = 0 COR = 1, maximum mathematical chirality (opposite shoes), for single crystals. Melt, solution, and gas phase host isolated achiral molecules (socks).

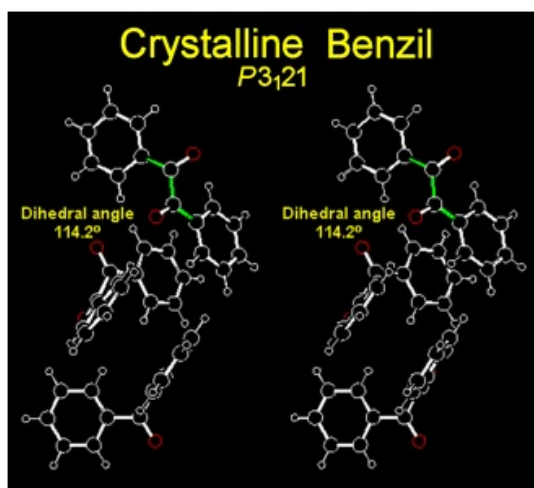


Figure 3: Crystalline benzil

Eötvös experiment detection threshold is 5×10^{-14} difference/average observing mass/mass divergence. Benzil's enthalpy of fusion, $\Delta H_{\text{fusion}} = 110.6 \text{ J/g}$ (G. D. Gatta, 2006) observes mc^2 mass-equivalent divergence. The diurnal sinusoidal EP component is Eq. (2.1) - (2.3),

$$\Delta E = (5 \times 10^{-17} \text{ kg/kg})(299,792,458 \text{ m/sec})^2 \text{ sensitivity mass-equivalent} \quad (2.1)$$

$$E = 4494 \text{ J/kg or } 4.494 \text{ J/g} \quad (2.2)$$

$$(4.494 \text{ J/g})/(110.6 \text{ J/g}) = 4.06\% \Delta \Delta H_{\text{fusion}} \quad (2.3)$$

Commercial differential scanning calorimeters (DSCs) have 0.1% precision. A geometric calorimetry experiment offers increased sensitivity to vacuum chiral anisotropy toward matter compared to a composition EP Eötvös experiment, Eq. (3), active mass fraction ratio multiplied by signal/instrument resolution,

$$(0.999713/0.0023974)(0.0406/0.001) = 16,900\times \text{ sensitivity,} \quad (3)$$

Two horizontally abutted DSCs' sample ports define a geographic north-south line. Each holds a ~3 mm diameter ~17 mg benzil single crystal sphere with sample carriers crimped against sublimation. One sample port consistently contains one crystal in space group $P3121$ and the other sample port one crystal in $P3221$. ΔH_{fusion} are simultaneously run. New crystals are run at half-hour intervals for 24 hours inclusive. Given sample geographic north-south alignment and Earth's inertial spin plus gravitational orbit angular momenta, a coordinate system is defined, cycling over 24 hours. For local geographic midnight - achiral, signal node; 0600 hrs - chiral, antinode; 1200 hrs - achiral, node; 1800 hrs - opposite chiral, opposite antinode for EP interaction.

Repeated the next day with east-west alignment. $\Delta\Delta H_{\text{fusion}}$ will have a six hour phase shift. ΔH_{fusion} of finely powdered racemic benzil is baseline, Fig. 4,



Figure 4: Crystalline to molten benzil transition

Case 1: $\Delta\Delta H_{\text{fusion}} = 0$. Zero net signal confirms vacuum achiral isotropy toward matter. $P3121$ and $P3221$ single crystal ΔH_{fusion} are identical to that of powdered racemic benzil. Values do not change versus time of day and samples' N-S or E-W geographic orientation.

Case 2: $\Delta\Delta H_{\text{fusion}} > 0$. Net non-zero signal confirms vacuum chiral anisotropy toward matter. Chemically identical enantiomorphous crystals, embedded within a resolved vacuum chiral background (opposite shoes on a left foot), melting into a common achiral state (socks), display different enthalpies of fusion. At least one ΔH_{fusion} will be different from that of powdered racemic benzil.

Case 3: $\Delta\Delta H_{\text{fusion}} \neq 0$, sinusoidally varying with time of day. The EP has a chiral geometric violation. The angle between Earth's inertial spin and gravitational orbit rotates $360^\circ/24$ hours. This sources a composition Eötvös experiment signal. Add $P3121$ and $P3221$ benzil test masses aligned N-S and the coordinate frame cycles chiral, achiral, opposite chiral, achiral every 24 hours.

Case 4: (Case 2)+(Case 3). The vacuum is chiral anisotropic toward chiral atomic mass distribution and the EP has a chiral geometric violation. Dark matter is in fact Milgrom acceleration, SUSY is fundamentally wrong, general relativity is in fact superset ECKS gravitation, quantum gravitation must be rederived to allow for chiral geometric EP violation. No prior observation in any venue at any scale is contradicted.

5. SPINNING OPPOSITE SHOES

Observe high resolution rotational spectra of a ~1 kelvin molecular beam racemic rotor mix. Isotropic vacuum elicits no chiral divergence, giving degenerate spectra. Trace chiral vacuum background splits enantiomers' energies (opposite shoes on a left foot) (Moffat, Six lectures on general fluid dynamics and two on hydromagnetic dynamo theory, 1977). Two rotational spectra, perhaps with unequal rotation temperatures, appear. Microwave (μ wave) and infrared (IR) spectrometries (dipole transitions) and Raman spectrometry (quadrupole transition) are diagnostic. Centripetal distortion induces a small dipole moment in some zero dipole moment symmetric molecules, e.g., tetrahedral methane spinning about its C_3 axis. Point group Oh sulfur hexafluoride spinning about its C_4 axis remains unpolarized, by symmetry, as do point group D_3 molecules spinning about their C_3 axes.

Required are rigid cage molecules with no pendent spinnable substituents. The EP is composition-inert. Chiral centers should be geometrically homochiral ignoring composition. Rotational symmetries render skeletal positions equivalent. Favor molecules with large CHI values in QCM software. Oblate symmetric tops have simplified rotational spectra. Good yield multi-gram syntheses afford μ wave, IR, and Raman samples. Pentacyclo[6.3.0.0^{2,6}.0^{3,10}.0^{5,9}]undecane, D_3 -trishomocubane, and derivatives (D. I. Sharapa 2012) (I. A. Levandovsky 2010) (W.-D. Fessner 1986) (G. J. Kent 1977) qualify, Fig. 5, Fig. 6, and Table 3. D_3 -trishomocubane has 8/11 skeletal atoms being explicit chiral centers. One C_3 plus three C_2 rotation axes define three unique skeletal positions: [4,7,11; achiral], [2,9; un-nameable chirality], [1,8,6,5,3,10; R-configuration displayed]

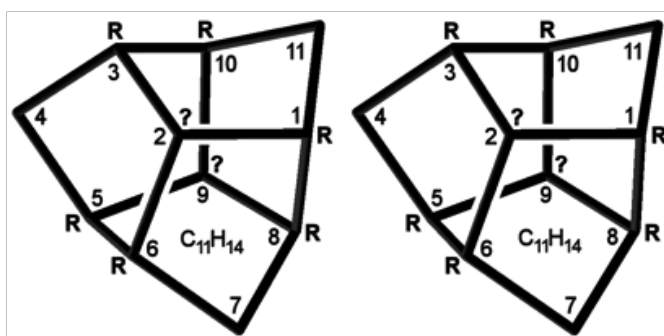


Figure 5: D_3 -trishomocubane, numbering and CIP chirality

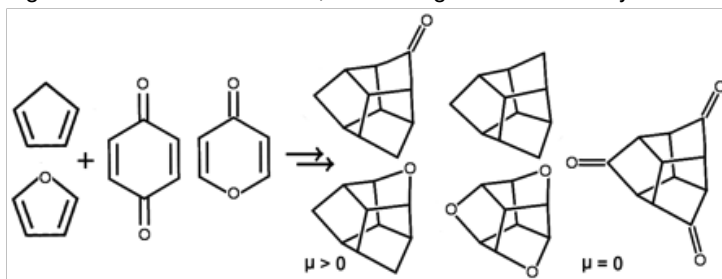


Figure 6: μ wave, IR; and Raman test molecules

Table 3: μ wave, IR; and Raman test molecules

Method	Molecule	Moments of Inertia, amu-Å			~ Dipole Moment	
					μ , D	
		I_x	I_y	I_z		
μ wave, IR	4-one	282.018			421.039	523.570
					3.0	HyperChem

μwave, IR	4-oxa	274.348	278.637	375.450	2.4 MARVIN
Raman	hydrocarbon	282.518	282.518	384.000	0.0 symmetry
Raman	4,7,11-trioxa	264.653	264.653	359.004	0.0 symmetry
Raman	4,7,11-trione	510.318	510.318	844.539	0.0 symmetry
Raman	fluorocarbon	1710.24	1710.24	2091.47	0.0 symmetry

Table 4 lists some test molecules' QCM outputs. CHI: normalized geometric chirality, 0 to 1. DSI: direct symmetry index, defined in (Petitjohn, 1999) section VI. 0 is best. COR: graph isomorphisms, "correspondences," 1 (identity) to unbounded integer. Smaller is better. Protein amino acid phenylalanine is chiral. Its α -carbon chiral center bears four very different groups: hydrogen, carboxyl, amino, and benzyl. QCM shows its 23 atoms in 3-space sum to small geometric chirality. 4-oxa-*D*3-trishomocubane's 23 atoms sum to a large CHI value, as do its isolated spin-0 atom skeleton and its isolated spin- $\frac{1}{2}$ hydrogens or fluorines. 4,7,11-trioxa-*D*3-trishomocubane's 19 atoms sum to a near-perfect geometrically chiral object.

Table 4: QCM-calculated geometric chiralities

Molecule	Moiety	CHI	DSI	COR
hydrocarbon	whole	0.628218	0.000000	48
	skeleton only	0.533027	0.000000	6
	hydrogens only	0.713354	0.000000	1
fluorocarbon	whole	0.649502	0.000000	48
	skeleton only	0.506504	0.000000	6
	fluorines only	0.758557	0.000000	1
4-oxa	whole	0.712524	0.000000	8
	skeleton only	0.542840	0.000000	2
	hydrogens only	0.800458	0.000000	1
4,7,11-trioxa-	whole	0.959321	0.000000	6
	skeleton only	0.484981	0.281997	4
	hydrogens only	0.562643	0.000000	6
phenylalanine	whole	0.058600	0.013103	8

5A. ROTATIONAL MICROWAVE AND INFRARED

Helium-entrained vapor of racemic ketone or ether is de Laval vacuum supersonic expanded, reducing rotation temperature to ~1 kelvin. The cryogenic molecular beam passes through a chirped-pulse FT μwave spectrometer (N. M. Kidwell, 2014) (I. A. Finneran, 2013) or FTIR spectrometer in kind to capture its high resolution rotational spectrum. Achiral isotropic vacuum displays enantiomers' degenerate indistinguishable spectra. Trace chiral anisotropic vacuum splits transition energies and/or rotor rotation temperatures, displaying non-degenerate one spectrum for each enantiomer, a left foot

bearing opposite shoes.

5B. ROTATIONAL RAMAN SPECTRA

Molecules lacking both a permanent and a centripetally-induced dipole moment display rotational spectra with high resolution Raman scattering. SF₆ centripetal distortion generates no dipole moment, but exquisite rotational spectra (V. Boudon L. M., 2014) (V. Boudon P. A., 2013) are obtained. *D3*-Trishomocubane has small anisotropic polarizability. Its 4,7,11-triketone and 4,7,11-trioxa derivatives have large anisotropic polarizabilities. Three synthetic approaches to the triketone are past literature (A. P. Marchand, 1987), contemporary methylene to carbonyl oxidations (M. S. Chen, 2010) (H. C. Tung, 1992), and 5-methylene-1,3-cyclopentadiene or 5-benzylidene-1,3-cyclopentadiene (for stability) starting material followed by oxidative cleavage to the carbonyl after photocyclization. The final carbonyl is placed by oxidation. 4,7,11-trioxa-*D3*-trishomocubane has near-perfect geometric chirality. Synthesis begins with furan plus pyrone rather than cyclopentadiene plus benzoquinone, placing 4,7-oxa-substitution. Follow with carbonyl oxidation I (e.g., Baeyer–Villiger) to the lactone, conversion of the carboxyl to a leaving group with ring opening and epimerization, then *endo*-alkoxide displacement.

Example: Phenyl (4-nitrophenyl, 2,4-dinitrophenyl, etc.) anion attack upon the lactone obtains the *endo*-alcohol plus base-promoted steric hindrance-driven α -carbon equilibrium inversion to the *exo*-phenylketone. 1,2-Ethanedithiol obtains the dithioketal, followed by dimethyldioxirane oxidation to the strongly electron-withdrawing disulfone (pKa ~12.5, and lowered by a nitrophenyl). *endo*-Alkoxide displacement at the α -carbon closes the ring ether by displacing the (nitro)phenyl disulfone anion.

5C. ESTIMATED SIGNAL AMPLITUDE

Boltzmann's constant offers vacuum coupling divergence detection for racemic molecular rotors as energy/mass, as rotational temperature. A one kelvin racemic molecular beam (pairs of shoes) is differentially sensitive to being embedded within vacuum resolved chiral anisotropy (left feet), Eq. (4.1) - (4.3). Differential energy misfits for 4-oxa-*D3*-trishomocubane (C₁₀H₁₂O; μ wave, IR) Eq. (4.4), *D3*-trishomocubane-4,7,11-trione (C₁₁H₈O₃; Raman) Eq. (4.5), and perfluoro-*D3*-trishomocubane (C₁₁H₁₄; Raman) Eq. (4.6) at Eötvös experiment detection threshold 5×10^{-14} difference/average observing mass/mass divergence are

$$(\Delta mc^2)/(\text{molar mass})/(\text{molecules/mole})(\text{Boltzmann's constant}) = \text{temperature} \quad (4.1)$$

$$(4.49378 \text{ J/g})(\text{molar mass})/(6.02214 \times 10^{23}/\text{mole})(1.38065 \times 10^{-23} \text{ J/kelvin}) \quad (4.2)$$

$$(0.540478)(\text{molar mass}) = \text{kelvins} \quad (4.3)$$

$$(0.540478) (148.202 \text{ g/mol}) = 80 \text{ kelvins, 4-oxa-}D3\text{-trishomocubane} \quad (4.4)$$

$$(0.540478) (188.179 \text{ g/mol}) = 101 \text{ kelvins, } D3\text{-trishomocubane-4,7,11-trione} \quad (4.5)$$

$$(0.540478) (398.095 \text{ g/mol}) = 215 \text{ kelvins, perfluoro-}D3\text{-trishomocubane} \quad (4.6)$$

Relative orientation of Earth's spin inertial acceleration and orbital gravitational acceleration varies sinusoidally over 24 hours. Given molecular beam geographic north-south alignment, for local geographic midnight - achiral, node; 0600 hrs - chiral, antinode; 1200 hrs - achiral, node; 1800 hrs - opposite chiral, antinode for EP interaction. Eötvös experiment minimum detectable divergence corresponds to large net outputs as μ wave, IR, and Raman racemate rotational temperature divergences even for modest coupling constants.

6. HISTORICAL PRECEDENT

Euclid is incomplete (cartography), then János Bolyai. Newtonian physics is incomplete, then relativity and quantum mechanics. The Dirac equation failed for proton magnetic moment (Otto Stern), then

quarks. Particle theory was mirror-symmetric, then Chen Ning Yang and Tsung-Dao Lee. Examine vacuum symmetry toward extreme enantiomorphic atomic mass distributions. Observe whether vacuum is rigorously achiral isotropic toward fermionic matter as it is toward boson photons. Nothing prohibits empirically falsifying a founding postulate, no matter how "obvious and logically true" it appears to be.

CONCLUSION

Three classes of chemical tests are presented to challenge a physics vacuum symmetry postulate. Existing bench top equipment can heal accumulated elegant but empirically inert quantum gravitation and supersymmetry theories. No prior observation in any venue at any scale would be contradicted by detected vacuum trace chiral anisotropy acting only upon hadrons. Untried geometric Eötvös, calorimetry, and rotational spectrometry are orders of magnitude more sensitive than zero net signal composition and spin Eötvös experiments. Some 45 years of speculation beginning with Leonard Susskind and Murray Gell-Mann in a 1970 Coral Gables, Florida stalled elevator can be reshaped in one day. Perform geometric tests of spacetime geometry, for the worst they can do is succeed.

WORKS CITED

- A. F. Palistrant, S. V. (1991). Enantiomorphism of three-dimensional space and line multiple antisymmetry groups. *Publ. Inst. Math., Nouv. Sér.* , 49 (63), 51- 60.
- A. M. Glazer, K. S. (1986). On the origin of optical activity in crystal structures. *J. Appl. Crystallogr.* , 19 (2), 108 - 122.
- A. P. Marchand, G. V. (1987). Syntheses of pentacyclo[5.4.0.02,6.03,10.05,9]undecane-4,8,11-trione, pentacyclo[6.3. 0.02,6.03,10.05,9]undecane-4,7,11-trione (D3-trishomocubane-trione), and. *J. Org. Chem.* , 52 (21), 4784-4788.
- D. I. Sharapa, I. A. (2012). Axial D3-trishomocubane derivatives with potential: dreams or reality? *Curr. Org. Chem.* , 16 (22), 2623 - 2651.
- Fritz, T. (2013). Velocity polytopes of periodic graphs and a no-go theorem for digital physics. *Discrete Math.* , 313 (12), 1289 - 1301.
- G. D. Gatta, M. J. (2006). Standards, calibration, and guidelines in microcalorimetry, Part 2. Calibration standards for differential scanning calorimetry. *Pure Appl. Chem.* , 78 (7), 1455 - 1476.
- G. J. Kent, S. A. (1977). Syntheses and relative stability of (D3)-trishomocubane (pentacyclo[6.3.0.02,6.03,10.05,9]undecane), the pentacycloundecane stabilomer. *J. Org. Chem.* , 42 (24), 3852 - 3859.
- H. C. Tung, C. K. (1992). Nature of the reactive intermediates from the iron-induced activation of hydrogen peroxide: agents for the ketonization of methylenic carbons, the monooxygenation of hydrocarbons, and the dioxygenation of aryl olefins. *J. Am. Chem. Soc.* , 114 (9), 3445 -3455.
- H.B. Nielsen, M. N. (1981). Absence of neutrinos on a lattice: (I). Proof by homotopy theory. *Nucl. Phys. B* , 185 (1), 20 - 40.
- I. A. Finneran, D. B. (2013). A direct digital synthesis chirped pulse Fourier transform microwave spectrometer. *Rev. Sci. Instrum.* , 84 (8).
- I. A. Levandovsky, D. I. (2010). The chemistry of D3-trishomocubane. *Russ. Chem. Rev.* , 79 (11), 1005 - 1026.
- J. Etxebarria, C. L. (2000). Origin of the optical activity of silver thiogallate. *Appl. Cryst.* , 33 (1), 126 - 129.

- M. S. Chen, M. C. (2010). Combined effects on selectivity in Fe-catalyzed methylene oxidation. *Science* , 327 (5965), 566 - 571.
- Moffat, H. K. Six lectures on general fluid dynamics and two on hydromagnetic dynamo theory. In R. B.-L. Peube (Ed.), *Fluid Dynamics* (pp. 151 - 233).
- Moffat, H. K. (1977). Six lectures on general fluid dynamics and two on hydromagnetic dynamo theory. In J.-L. P. R. Balian (Ed.), *Fluid Dynamics* (pp. 175 - 176). Gordon and Breach.
- N. M. Kidwell, V. V.-V. (2014). Chirped-pulse fourier transform microwave spectroscopy coupled with a flash pyrolysis microreactor: structural determination of the reactive intermediate cyclopentadienone. *J. Phys. Chem. Lett.* , 5 (13), 2201 - 2207.
- N. P. Pitjev, E. V. (2013). Constraints on dark matter in the solar system. *Astron. Lett.* , 39 (3), 141 - 149.
- Petitjohn, M. (1999). On the root mean square quantitative chirality and quantitative symmetry measures. *J. Math. Phys.* , 40 (9), 4587 - 4595.
- S. Yamaguchi, H. S. (1973). Asymmetric reductions with chiral reagents from lithium aluminum hydride and (+)-(2S,3R)-4-dimethylamino-3-methyl-1,2-diphenyl-2-butanol. *J. Org Chem.* , 38 (10), 1870 - 1877.
- Souvignier, B. (2003). Enantiomorphism of crystallographic groups in higher dimensions with results in dimensions up to 6. *Acta Cryst. A* , 59 (3), 210 - 220.
- T. A. Wagner, S. S. (2012). Torsion-balance tests of the weak equivalence principle. *Class. Quantum Grav.* , 29 (18), 184002.
- V. Boudon, L. M. (2014). Resolving the forbidden band of SF₆. *Phys. Chem. Chem. Phys.* , 16 (4), 1415 - 142.
- V. Boudon, P. A. (2013). High-resolution spectroscopy and analysis of the v₂ + v₃ combination band of SF₆ in a supersonic jet expansion. *Molec. Phys.* , 111 (14 - 15), 2154 - 2162.
- W.-D. Fessner, H. P. (1986). D₃-trishomocubane trione synthesis and optical resolution. *Tetrahedron* , 42 (6), 1797 - 1803.